Dynamic Processes and Active Power Control of Hydropower Plants

Weijia Yang

杨威嘉

UPPSALA
UNIVERSITET

Abstract

Hydro-electricity plays an important role in the safe, stable and efficient operation of electrical power systems. The performance of hydropower plants in terms of frequency control is more and more important. Besides, in recent years, wear and tear of hydropower turbines is increasing, due to more regulation movements caused by the increasingly more integration of intermittent renewable energy sources. Hence, the research on wear and tear of hydro units is exceedingly necessary.

A sophisticated mathematical model of hydropower units is presented. Based on one Swedish hydropower plant and three Chinese plants, simulations and on-site measurements are compared for different operating conditions. The main error in each simulation is also discussed in detail. Then, for the grid-connected operation, general rules for controlling the power response time are investigated. A response time formula is deduced to predict the power response and supply a flexible guidance of parameter tuning. The factors which affect the power response time are investigated from aspects of both regulation and water way system properties. For the isolated operation, stabilizing the low frequency oscillation of hydropower plants caused by surge fluctuation is studied. Frequency stability under power control is compared with frequency control, by adopting the Hurwitz criterion and numerical simulations.

In terms of the wear and tear of the hydro turbine, a comprehensive discussion on the influence of primary frequency control is conducted by applying numerical simulations and a concise theoretical derivation. The results show the influences from different factors, e.g. governor parameters, power feedback mode and nonlinear governor factors. Then, the use of a controller filter is proposed as a solution of the trade-off between reducing the wear of turbines and maintaining the regulation performance, reflected by the frequency quality of the power system. The widely used dead zone is compared with a floating dead zone and a linear filter, by time domain simulation and frequency domain analysis.

The results supply the understanding of the modeling and analysis of the dynamic processes in hydropower systems, and the suggestions of the control strategies of hydropower plants in different operating conditions under the stability requirements of power systems.

There is no elevator to success.
You have to take the stairs.

List of Papers

This thesis is based on the following papers, which are referred to in the text by their Roman numerals.

I **Weijia Yang**, Jiandong Yang, Wencheng Guo, Per Norrlund. "Response time for primary frequency control of hydroelectric generating unit". *International Journal of Electrical Power & Energy Systems*, 74(2016):16–24.

II **Weijia Yang**, Jiandong Yang, Wencheng Guo, Per Norrlund. "Frequency stability of isolated hydropower plant with surge tank under different turbine control modes". *Electric Power Components and Systems*, 43(15): 1707-1716.

III **Weijia Yang**, Jiandong Yang, Wencheng Guo, Wei Zeng, Chao Wang, Linn Saarinen and Per Norrlund. "A mathematical model and its application for hydro power units under different operating conditions". *Energies*, **2015**, *8*(9), 10260-10275.

IV **Weijia Yang**, Per Norrlund, Linn Saarinen, Jiandong Yang, Wencheng Guo, Wei Zeng. "Wear and tear on hydro power turbines – influence from primary frequency control". *Renewable Energy* (*minor revisions*)*,* September 2015.

V **Weijia Yang**, Per Norrlund, Linn Saarinen, Jiandong Yang, Wei Zeng, Urban Lundin. "Wear reduction for hydro power turbines considering frequency quality of power systems: a study on controller filters", *Submitted to IEEE Transactions on Energy Conversion,* September 2015.

Reprints were made with permission from the respective publishers. The author has further contributed to the following papers, not included in this thesis:

VI Wencheng Guo, Jiandong Yang, **Weijia Yang**, Jieping Chen, Yi Teng. "Regulation quality for frequency response of turbine regulating system of isolated hydroelectric power plant with surge tank". *International Journal of Electrical Power & Energy Systems*, 73(2015): 528-538.

VII Wencheng Guo, Jiandong Yang, Jieping Chen, **Weijia Yang**, Yi Teng, Wei Zeng. "Time response of the frequency of hydroelectric generator unit with surge tank under isolated operation based on turbine regulating modes". *Electric Power Components and Systems, accepted (in production)*.

VIII Jiandong Yang, Wei Zeng, **Weijia Yang**, Shangwu Yao, Wencheng Guo. "Runaway stabilities of pump-turbines and its correlations with S-shaped characteristic curves" (in Chinese), *Transactions of the Chinese Society for Agricultural Machinery*, 46(2015): 59-64.

IX Jiandong Yang, Huang Wang, Wencheng Guo, **Weijia Yang**, Wei Zeng. "Simulation of wind speed in the ventilation tunnel for surge tank in transient process", *Submitted to Journal of Hydrodynamics*.

X Wei Zeng, Jiandong Yang, **Weijia Yang**, Wencheng Guo, Jiebin Yang. "Instability analysis of pumped-storage stations at no-load conditions using a parameter-varying model", *manuscript.*

A graphical introduction of the topics in the thesis is shown below.

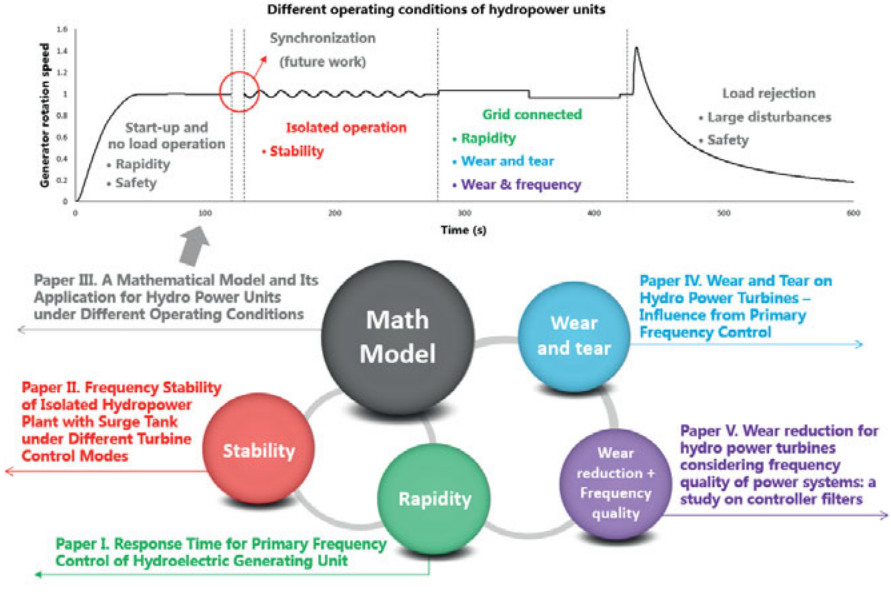

Contents

Abbreviations and symbols

Abbreviation	Description
HPP	hydropower plant
PFC	primary frequency control
GV	guide vane
GVO	guide vane opening
SISO	single-input and single-output
PID	proportional-integral-derivative
PI	proportional-integral

List of symbols in subsection 2.1.1:

Symbol	Description
a	velocity of pressure wave
A	cross-sectional area of pipeline
D	inner diameter of the pipe
D_1	diameter of runner
e_g	coefficient of load damping
f	Darcy-Weisbach coefficient of friction resistance
f_c	given frequency
f_g	generator frequency
g	gravitational acceleration
H	piezometric water head in the pipeline
H_p	piezometric water head of turbine inlet
H_s	piezometric water head of turbine outlet
J	moment of inertia
M_{11}	unit moment
M_g	resistance moment of generator
M_t	mechanical moment of turbine
n_{11}	unit rotational speed
n	rotational speed
n_c	given rotational speed
n_r	rated rotational speed
p_c	given power
p_r	rated power output
p_g	generator power
Q_p	discharge of turbine inlet

Q_s	discharge of turbine outlet
Q_{11}	unit discharge
t	time
V	average flow velocity of pipeline section
x	position
x_f	relative value of speed (frequency) deviation, $x_f = (f_g - f_c) / f_c$
y	guide vane opening (servomotor stroke)
y_c	given opening
y_{PID}	opening deviation after PID terms
y_{servo}	opening deviation after servo block
θ	angle between axis of pipeline and horizontal plane
Δn	speed deviation
ΔH	$\Delta H = \left(\frac{\alpha_P}{2gA_P^2} - \frac{\alpha_S}{2gA_S^2} \right) Q_P^2$
α_P	correlation coefficient of kinetic energy at turbine inlet
α_S	correlation coefficient of kinetic energy at turbine outlet
A_P	cross-sectional area of turbine inlet
A_S	cross-sectional area of turbine outlet

List of symbols in subsection 2.1.2:

Symbol	**Description**
$q_y = \frac{Q_y - Q_{y0}}{Q_{y0}}$	discharge of draw water tunnel
$q_t = \frac{Q - Q_0}{Q_0}$	discharge of turbine
$x = \frac{f_g - f_c}{f_c}$	rotational speed of turbine
$y = \frac{Y - Y_0}{Y_0}$	guide vane opening
$m_t = \frac{M_t - M_{t0}}{M_{t0}}$	dynamic moment of turbine
$m_g = \frac{M_g - M_{g0}}{M_{g0}}$	braking moment of generator
$p_g = \frac{P_g - P_{g0}}{P_{g0}}$	power of hydroelectric generating unit
$p_c = \frac{P_c - P_{c0}}{P_{c0}}$	given power of hydroelectric generating unit
$z = \frac{\Delta Z}{H_0}$	relative change value of water level in surge tank

Symbols from q_y to z are relative values (per unit values), and symbols with subscript "0" stands for initial value.

ΔZ	absolute change value of water level in surge tank
H_0	net head of turbine
h_{yo}	head loss of draw water tunnel
T_{wy}	water inertia time constant of draw water tunnel
$T_F = \frac{FH_0}{Q_{y0}}$	surge tank time constant
F	cross section area of surge tank
T_a	generating unit inertia time constant
e_h, e_x, e_y	moment transmission coefficients of turbine
e_{qh}, e_{qx}, e_{qy}	discharge transmission coefficients of turbine
e_g	coefficient of load damping
K_p, K_i, K_d, T_y, b_p, e_p	governor parameters

1 Introduction

Hydro-electricity plays an important role in the safe, stable and efficient operation of electric power systems. Frequency stability of power systems refers to the ability to maintain steady frequency following a severe system upset resulting in a significant imbalance between generation and load. In order to suppress power grid frequency fluctuations, generating units change their power output automatically according to the change of grid frequency, to make the active power balanced again. This is the primary frequency control (PFC). PFC of electrical power grids is commonly performed by units in hydropower plants (HPPs), because of the great rapidity and amplitude of their power regulation.

A hydropower generation system is a complex nonlinear power system including hydraulic, mechanical, electrical and magnetic subsystems. Nowadays, the size of HPPs and the structure complexity of systems have been increasing, especially in China. The proportion of electricity generated by intermittent renewable energy sources have also been growing. Therefore, the performance of HPPs in terms of frequency control is more and more important. The research on control strategies and dynamic processes of HPPs is of great importance. The frequency stability of hydropower units is a critical factor of power system security and power quality. The power response time for evaluating the frequency regulation quality, is also a key indicator.

In recent years, there is a tendency that the new turbines experience fatigue to a greater extent than what seem to be the case for new runners decades ago, due to more regulation movements caused by increasingly more integration of intermittent renewable energy sources. In some countries, as in Sweden, PFC is a service that the transmission system operator buys from the power producers. In other countries, as in Norway and China, there is also an obligation for the producers to deliver this service, free of charge. However, there are costs related to this, e.g. due to design constraints and auxiliary equipment when purchasing a new unit or system, and due to wear and tear which affects the expected life time and maintenance intervals. Hence the specific research on wear and tear of hydro units due to PFC is exceedingly necessary.

1.1 Previous research

1.1.1 Dynamic processes and modeling of hydropower plants

An IEEE working group [1] and Jaeger [2] proposed the hydraulic system modeling method and further investigated of the interactions between power system oscillation and the dynamic characteristics of the hydraulic-mechanical system. Souza Jr. [3], Fang [4] and Zeng [5] have constructed non-linear models for the transient processes of the HPPs with a focus on the influence of the surge tank. Strah [6] proposed an integrated system analysis model with respect to the rotational speed and active power control during hydropower plant operation.

Nicolet [7, 8] built a high-order model of hydropower plants in islanded power networks and studied unsteady operation of hydroelectric systems. Jones [9] established a refined model for pumped storage power plant, studied the nonlinear, multivariable and time-variant system characteristics, and intensively explored the power oscillation issue based on a pumped storage power plant in Britain. Perez-Diaz [10] established an operating model for grid-connected pumped storage power plants, and probed into hydraulic short-circuit characteristics. Kishor [11] extensively reviewed research results in modeling, control strategies, as well as regulation and operation performance for HPPs.

1.1.2 Regulation quality and operating stability

Jones published a book on the operational control strategies for hydropower plant [12]. Wei wrote a Chinese book focused on turbine speed regulator and load frequency control for the power grid [13]. These two books indeed have comprehensive information and research results which are very helpful.

Doctoral dissertations of Fu [14] and Bao [15] mainly involve the regulation performance and stability of hydropower plant with surge tank. Saarinen [16] studied the flexibility demand and grid frequency control from the hydropower perspective.

Chen [17] looked into the modeling and control strategies for nonlinear systems of hydropower plants with surge tanks, based on state-space equations. Cebeci [18] explored the effect of the speed regulator settings of the hydroelectric generator sets on the frequency stability of the power grid in Turkey. Pico [19] conducted in-depth analysis on the very low frequency oscillations observed in the Colombian power grid in the 0.05-Hz range. In view of the oscillation issue of frequency ranging from about 0.011 to 0.017 Hz in the northern European electric power system, Grøtterud [20] established a SIMPOW-based hydropower plant model, and conducted numeric analysis for the power grid in Norway and Sweden.

1.1.3 Wear and tear

In the field of tribology, Ukonsaari [21], Gawarkiewicz [22] and Simmons [23] have conducted studies from the perspective of tribology to investigate the mechanism of wear and tear of guide vane bearings during the operation of the hydroelectric generator set.

In the fields of hydraulics and hydrodynamics, Gagnon [24] studied the effect of generator set startup strategies on the service life of the Francis turbine runner. Doujak [25] discussed the influence of an increasingly growing share of solar power and wind power integrated into the power grid on the operation and maintenance of the hydropower system. In a comprehensive review, Trivedi [26] elaborated the effect of the transient process during the operation of the hydroelectric generator set on the service life of the Francis turbine runner. Storli [27] and Seidel [28] discussed dynamic loads on Francis runners and their impact on fatigue life.

More specific and detailed discussions on the previous research can be found in the background sections of Paper I -V.

1.2 Outline of this thesis

In Chapter 2, the theoretical foundations of the research in this thesis are briefly introduced.

In Chapter 3, different operating conditions of hydropower plants is discussed, based on Paper III. The response time for PFC (grid-connected operation) and the frequency stability of isolated operation are studied, based on Paper I and II.

In Chapter 4, wear and tear of hydropower turbines is investigated from PFC respective, based on Paper IV. Then, controller filters are studied to reduce the wear and tear, and the frequency quality of power systems is considered as a trade-off factor. This work connects to Paper V.

In Chapter 5, the conclusions of the thesis are summarized, and the future work of the PhD program is presented in Chapter 6.

2 Theory

In this chapter, the theoretical foundations of this thesis are presented briefly. In section 2.1, various mathematical models of hydropower plants, which are the fundamental of this thesis, are presented. In section 2.2, the basic theory of the Laplace transform and transfer functions is introduced, and they are applied in the governor equation analysis in the studies of the response time and wear of the turbine. In section 2.3, the Routh–Hurwitz criterion is presented, and it is adopted for analyzing the frequency stability in section 3.3. In section 2.4, the Nyquist stability criterion and the describing function method are introduced, and they are applied for analyzing the frequency stability in section 4.3. Section 2.2 – 2.4 are based on two books, [29] and [30].

2.1 Modeling of hydropower plants

In this section, different models of hydropower plants for different study purposes in this thesis are introduced.

2.1.1 Sophisticated model for numerical simulation

Based on Paper III, a mathematical model of hydropower units, especially a governor system model for different operating conditions, is presented in this subsection based on the existing basic version of software TOPSYS [15, 31] by applying Visual C++. Models of other components (e.g. pipeline system) in the HPP system are only shortly presented, more details can be found in [15]. This model is the base of most numerical simulations of this thesis. The graphical user interface of TOPSYS is shown in Figure 2.1.

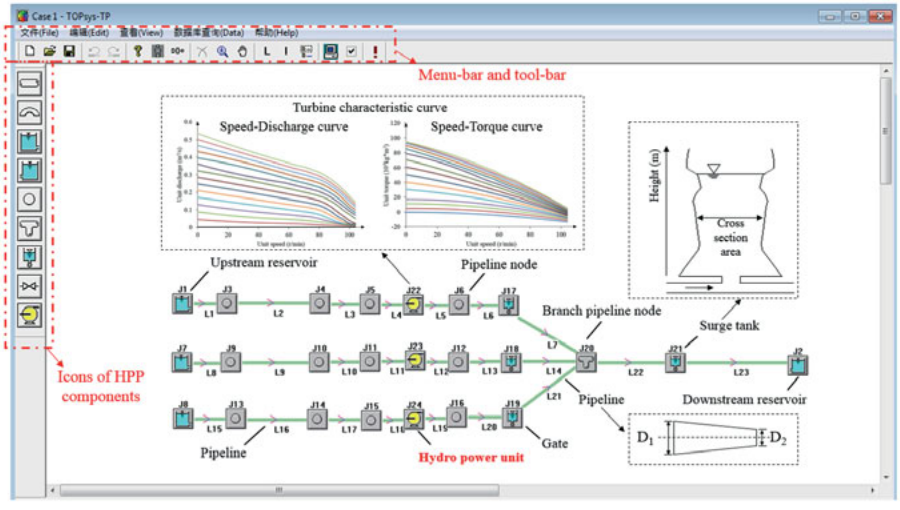

Figure 2.1. Graphical user interface of TOPSYS and a model of a Swedish HPP (Case 1 in Chapter 3)

In the basic version of TOPSYS, the model of waterway systems and hydraulic turbines has the following characteristics. (1) Equations for compressible flow are applied in the draw water tunnel and penstock, considering the elasticity of water and pipe wall. (2) Different types of surge tanks and tunnels are included. (3) Characteristic curves of the turbine are utilized, instead of applying simplified transmission coefficients. These characteristics lay a solid foundation for this study to achieve efficient and accurate simulation results.

- Pipeline system:

The continuity equation is

$$V\frac{\partial H}{\partial x}+\frac{\partial H}{\partial t}+\frac{a^2}{g}\frac{\partial V}{\partial x}+\frac{a^2V}{gA}\frac{\partial A}{\partial x}-\sin\theta\cdot V=0\,. \tag{2.1}$$

The momentum equation is

$$g\frac{\partial H}{\partial x}+V\frac{\partial V}{\partial x}+\frac{\partial V}{\partial t}+f\frac{V|V|}{2D}=0\,. \tag{2.2}$$

The details of all the symbols in this subsection can be found in the Abbreviations. The elastic water hammer effect is considered and different forms of pipelines, channels and surge tanks are included in the model.

- Turbine:

In this thesis, the Francis turbine is discussed. Figure 2.2 illustrates some of the notation.

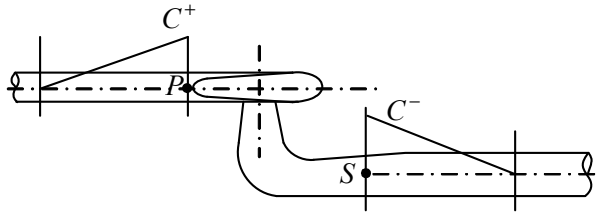

Figure 2.2. Illustration of the Francis turbine model

The equations of the models are shown below. Continuity equation is

$$Q_S = Q_P . \tag{2.3}$$

The equations of the method of characteristics are

$$\mathrm{C}^{+}\colon\ Q_P = C_P - B_P H_P . \tag{2.4}$$

$$\mathrm{C}^{-}\colon\ Q_S = C_M + B_M H_S . \tag{2.5}$$

The flow equation of turbine is

$$Q_P = Q_{11}\, D_1^2 \sqrt{\left(H_P - H_S\right) + \Delta H} . \tag{2.6}$$

The equations of unitary parameters are

$$n_{11} = nD_1 / \sqrt{\left(H_P - H_S\right) + \Delta H} \tag{2.7}$$

$$M_t = M_{11}\, D_1^3 \left(H_P - H_S + \Delta H\right) . \tag{2.8}$$

Characteristic curve equations of turbine are

$$Q_{11} = f_1\left(n_{11}, Y\right) \tag{2.9}$$

$$M_{11} = f_2\left(n_{11}, Y\right), \tag{2.10}$$

where functions f_1 and f_2 represent the interpolation of the characteristic curves of the turbine. The equation

$$p_g = M_t \frac{\pi n}{30} \tag{2.11}$$

describes the transform from torque to power output.

● Generator:

For the generator modeling, the first-order swing equation is adopted. For the single-machine isolated operation, the equation has the general form, as shown in

$$\mathrm{J}\frac{\pi}{30}\frac{dn}{dt} = M_t - M_g - \frac{30 e_g p_r}{n_r^2 \pi}\Delta n . \tag{2.12}$$

For the single-machine to infinite bus operation, it is assumed that the rotation speed is constant at the rated value or some other given values, yielding

$$n = n_c\left(f_g = f_c\right). \tag{2.13}$$

Under the off-grid operation, the values of M_g and e_g are 0, and the corresponding equation

$$J\frac{\pi}{30}\frac{dn}{dt}=M_t \tag{2.14}$$

can be considered as a special case of (2.12). The generator frequency, f_g, is transferred from the speed, n.

● Governor system in TOPSYS:

The governor equation has various expressions under different operating conditions and control modes. Figure 2.3 demonstrates the complete control block diagram of the proportional-integral-derivative (PID) governor system. The main non-linear factors (dead-zone, saturation, rate limiting and backlash) are included. All the variables in the governor system are per unit values. The S_1, S_2 and S_3 blocks are selectors between different signals, and the zero input to the selector means no input signal.

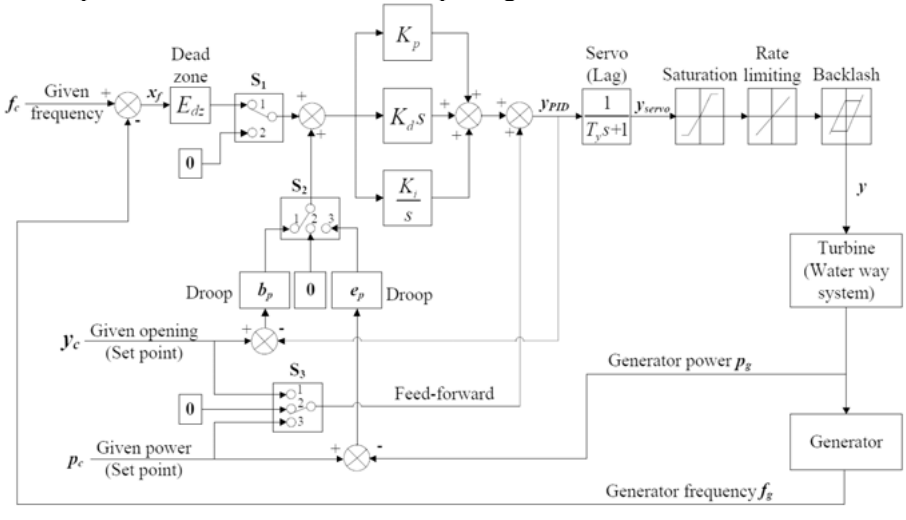

Figure 2.3. Block diagram of the governor system

For the normal operation, which means the isolated and the grid-connected operation with load, there are three main control modes: frequency control, opening control and power control. This study establishes a governor model with the switchover function of control mode.

In the frequency control mode, as shown in Figure 2.3, the feedback signal contains not only the frequency value, but also the opening or power, which forms the frequency control under opening feedback and power feedback, as respectively shown in

$$\begin{aligned} b_p K_d \frac{dy_{PID}^{\ 2}}{d^2t}+(1+b_p K_p)\frac{dy_{PID}}{dt}+b_p K_i y_{PID} \\ =-\left(K_d \frac{dx_f^{\ 2}}{d^2t}+K_p \frac{dx_f}{dt}+K_i x_f\right), \end{aligned} \tag{2.15}$$

$$e_p K_d \frac{dp_t^{\,2}}{d^2 t} + e_p K_p \frac{dp_t}{dt} + e_p K_i (p_g - p_c) + \frac{dy_{PID}}{dt} = -\left(K_d \frac{dx_f^{\,2}}{d^2 t} + K_p \frac{dx_f}{dt} + K_i x_f \right). \quad (2.16)$$

The symbols in governor equations are illustrated in Figure 2.3. In the opening control mode, the governor controls the opening according to the given value (y_c). As demonstrated by Figure 2.3, the opening control is equivalent to the frequency control under the opening feedback without the frequency deviation input (x_f). The equation of the opening control is

$$b_p K_d \frac{dy_{PID}^{\,2}}{d^2 t} + (1 + b_p K_p) \frac{dy_{PID}}{dt} + b_p K_i y_{PID} - \frac{dy_c}{dt} = 0. \quad (2.17)$$

Besides, the modeling of the opening control process can be simplified by ignoring the engagement of the PID controller, i.e. setting the opening directly equal to the given value, as shown in

$$y_{PID} = y_c. \quad (2.18)$$

In the power control mode, the governor controls the opening according to power signals, leading the power output to achieve the given value. The equation is

$$e_p K_d \frac{d(p_g - p_c)^2}{d^2 t} + e_p K_p \frac{d(p_g - p_c)}{dt} + e_p K_i (p_g - p_c) - \frac{dp_c}{dt} + \frac{dy_{PID}}{dt} = 0. \quad (2.19)$$

It is worth noting that a simpler controller, without the proportional (P) and derivative (D) terms, is applied in many real HPPs, as shown in

$$e_p K_i (p_g - p_c) - \frac{dp_c}{dt} + \frac{dy_{PID}}{dt} = 0. \quad (2.20)$$

Discussion of equations for start-up, no-load operation, emergency stop and load rejection can be found in Paper III. In the governor equations (2.15) – (2.20), only the value of y_{PID} is solved for. For the servo part, the output opening (y_{servo}) is found by solving

$$y_{PID} = T_y \frac{dy_{servo}}{dt} + y_{servo}. \quad (2.21)$$

Then, the value of final opening (y) is the value after the non-linear functions i.e. dead-zone, saturation, rate limiting and backlash. The selectors (S_1, S_2 and S_3) in the governor system are related to each other. Table 2.1 shows various states of selectors in different control modes. Table 2.2 concludes the equation set, in this study, of hydropower units under different operating conditions.

Table 2.1. Status of selectors in different control modes

Control mode	Equation	S_1 status	S_2 status	S_3 status
Frequency control	(2.15)	1	1	2
	(2.16)	1	3	2
Opening control	(2.17)	2	1	1
	(2.18)	2	2	1
Power control	(2.19)	2	3	3
	(2.20)	2	2	3

Table 2.2. Equation set of the hydropower unit under different operating conditions

Operating condition		Equation set		
		Governor	Generator	Turbine
Normal operation	Frequency control	(2.15) or (2.16)	(2.12) or (2.13)	(2.3)-(2.10)
	Opening control	(2.17) or (2.18)	(2.12) or (2.13)	
	Power control	(2.19) or (2.20)	(2.12) or (2.13)	
Start-up	Open-loop	(2.18)	(2.14)	
	Closed-loop	(2.15)	(2.14)	
No-load operation		(2.15)	(2.14)	
Emergency stop		(2.18)	(2.14)	
Load rejection		(2.15)	(2.14)	

2.1.2 Simplified model for theoretical derivation

The simplified model for theoretical derivation is mainly for the stability analysis in Paper II. Comparing to the TOPSYS model, this linearized model is on the basis of following assumptions: (1) Rigid water hammer equations are adopted in the draw water tunnel, neglecting the elasticity of water and pipe wall. (2) The equation of the penstock is ignored. (3) Head loss at the bottom of surge tanks is not considered. (4) Steady-state characteristic of the hydraulic turbine is described by transmission coefficients. (5) Nonlinear characteristics of the governor (saturation, rate limiting and dead zone) are ignored. The basic equations are indicated in the schematic diagram shown in Figure 2.4.

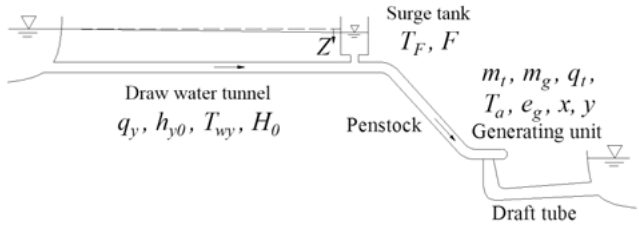

Figure 2.4. Schematic diagram for the simplified model: water way and power generation system in a HPP with surge tank

The dynamic equation of the draw water tunnel is

$$z - \frac{2h_{y0}}{H_0} q_y = T_{wy} \frac{dq_y}{dt} \ . \tag{2.22}$$

The continuity equation of the surge tank is

$$q_y = q_t - T_F \frac{dz}{dt} \ . \tag{2.23}$$

The moment and discharge equations of the hydraulic turbine are

$$m_t = -e_h z + e_x x + e_y y \tag{2.24}$$

$$q_t = -e_{qh} z + e_{qx} x + e_{qy} y \ . \tag{2.25}$$

The generator equation is

$$T_a \frac{dx}{dt} = m_t - (m_g + e_g x) \ . \tag{2.26}$$

The governor equation for frequency control is

$$\begin{aligned} (T_y + b_p K_P T_y) \frac{\mathrm{d}^2 y}{\mathrm{d}t^2} + (1 + b_p K_P + b_p K_I T_y) \frac{\mathrm{d}y}{\mathrm{d}t} \\ + b_p K_I y = -(K_P \frac{\mathrm{d}x}{\mathrm{d}t} + K_I x) \end{aligned} \ . \tag{2.27}$$

The governor equation for power control is

$$T_y \frac{\mathrm{d}^2 y}{\mathrm{d}t^2} + \frac{\mathrm{d}y}{\mathrm{d}t} = \frac{\mathrm{d}p_c}{\mathrm{d}t} + e_p K_I (p_c - p_g) \ . \tag{2.28}$$

The details of all the symbols in this subsection 2.1.2 can be found in the Abbreviations. Comparing to the governor equations (2.15) and (2.20) in the simulation model, governor equations here include the parameter T_y, and ignore the governor parameter K_d.

2.1.3 Lumped model for study from system perspective

This subsection is for the study from the system perspective in section 4.3, which is based on based on Paper V.

- Model for time-domain simulation:

In order to take the power system perspective into account, a MATLAB/Simulink model [16, 32] of the Nordic power system is applied, as shown in Figure 2.5.

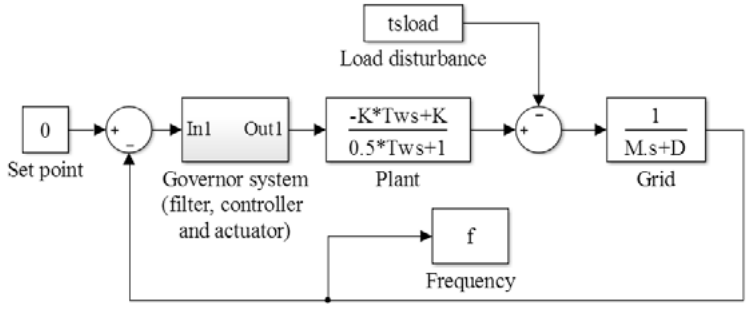

Figure 2.5. Simulink model of the Nordic power system, for computing the power system frequency. The governor system is shown in Figure 2.6.

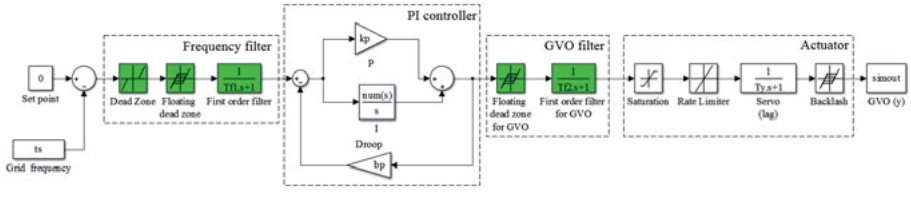

Figure 2.6. The Simulink model of a general governor system with different filters, for computing guide vane (GV) movements. The blocks of the filters are highlighted in green.

In the model, all the power plants are lumped into one. The equations of the proportional-integral (PI) controller, the plant and the grid are shown in

$$\text{PI controller: } C(s) = \frac{K_p s + K_i}{\left(1 + b_p K_p\right) s + b_p K_i}, \tag{2.29}$$

$$\text{Plant: } P(s) = K \cdot \frac{-T_w s + 1}{0.5 T_w s + 1}, \tag{2.30}$$

$$\text{Grid: } G(s) = \frac{1}{Ms + D}. \tag{2.31}$$

Here, the K_p, K_i and b_p are controller parameters. The setting values of the dead zone, floating dead zone for frequency and floating dead zone for guide vane opening (GVO) are E_{dz}, E_{fdz} and E_{fdz2} respectively. The identified parameters of the plant and the grid are given in Table 2.3. The governor system components (filter, PI controller and actuator) are expressed in a subsystem for decreasing the figure size. The details are found in Paper V.

Table 2.3. Parameters of the plant and the grid

Symbol	Parameter	Value
K	Steady state gain	$10\times b_p$ pu
T_w	Water time constant	1.5 s
M	System inertia	13 s
D	Load damping constant	0.5 pu

● Model for frequency-domain analysis:

The block diagram of the power system, for frequency domain analysis, is shown in Figure 2.7.

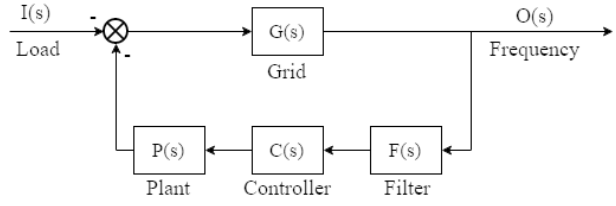

Figure 2.7. Block diagram of the power system model for frequency domain analysis

Comparing to the time domain model, the non-linear part of the actuator is ignored here. The transfer functions of the PI controller, the plant and the grid are shown in (2.29) though (2.31). The term $F(s)$ is a general transfer function for the filter. It is replaced by specific transfer functions of different filters according to the case. In the frequency analysis, the position of the filter (before or after the controller) does not affect the result. The transfer functions of the first-order linear filters are

$$F_{f1}(s)=\frac{1}{T_{f1}\cdot s+1}, \tag{2.32}$$

$$F_{f2}(s)=\frac{1}{T_{f2}\cdot s+1}. \tag{2.33}$$

Here, the parameters T_{f1} and T_{f2} are known as the filter time constants of the frequency filter and the GVO filter respectively in Figure 2.6.

For investigating the stability of the system, the open-loop systems with different filters are examined by the Nyquist stability criterion. Transfer functions of these systems are found in Paper V. In order to analyze the non-linear filters in frequency domain, the describing function method is applied. The describing function of a dead zone of size E_{dz} [30] is

$$N_{dz}(A)=\frac{1}{\pi}\left[\pi-2\arcsin\left(\frac{E_{dz}}{A}\right)-2\left(\frac{E_{dz}}{A}\right)\sqrt{1-\left(\frac{E_{dz}}{A}\right)^2}\right]\left(A>E_{dz}\right). \tag{2.34}$$

The describing function of a floating dead zone of size E_{fdz} (backlash) [30] is

$$N_{fdz}(A)=\frac{1}{\pi}\left[\frac{\pi}{2}+\arcsin\left(1-\frac{E_{fdz}}{A}\right)+\left(1-\frac{E_{fdz}}{A}\right)\sqrt{\frac{2E_{fdz}}{A}-\left(\frac{E_{fdz}}{A}\right)^2}\right] \\ -j\frac{1}{\pi}\left[\frac{2E_{fdz}}{A}-\left(\frac{E_{fdz}}{A}\right)^2\right]\left(A>E_{fdz}\right) \quad (2.35)$$

Here, the parameter A means the amplitude of the periodical input signal. The basic theory of the Nyquist criterion and the describing function method is presented in section 2.4.

2.2 Laplace transform and transfer function

This section is based on [29], to explain the basic theory of the Laplace transform and the transfer function.

● Laplace transform and inverse Laplace transform:

One purpose of the Laplace transform is to solve linear ordinary differential equations, through three steps below: (1) Converting the differential equations into an algebraic equation in *s*-domain; (2) dealing with the simple algebraic equation; (3) taking the inverse Laplace transform to acquire the solution. The mathematical definition of the Laplace transform and the inverse Laplace transform can be found in [29].

● Transfer function (single-input and single-output, SISO):

For a linear time-invariant SISO system *G(s)*, the definition of a transfer function of it is

$$G(s)=\mathcal{L}\left[g(t)\right], \quad (2.36)$$

and all the initial conditions set to zero. Here, $\mathcal{L}$ means the Laplace transform, and *g(t)* is the impulse response with the scalar functions input *u(t)* and output *y(t)*. The relationship between the Laplace transforms is shown in

$$G(s)=\frac{Y(s)}{U(s)}, \quad (2.37)$$

and all the initial conditions set to zero. Here, *Y(s)* and *U(s)* are the Laplace transforms of *y(t)* and *u(t),* respectively.

For a following *n*th-order differential equation with constant real coefficients

$$\frac{d^n y(t)}{dt^n}+a_{n-1}\frac{d^{n-1}y(t)}{dt^{n-1}}+\ldots+a_1\frac{dy(t)}{dt}+a_0 y(t) \\ =b_m\frac{d^m u(t)}{dt^m}+b_{m-1}\frac{d^{m-1}u(t)}{dt^{m-1}}+\ldots+b_1\frac{du(t)}{dt}+b_0 u(t) \quad (2.38)$$

after simply taking the Laplace transform of both sides of the equation and assuming zero initial conditions, the transfer function of the linear time-invariant system is obtained, as shown in

$$\begin{aligned}&\left(s^n + a_{n-1}s^{n-1} + \ldots + a_1 s + a_0\right) Y(s) \\ &\quad = \left(b_m s^m + b_{m-1}s^{m-1} + \ldots + b_1 s + b_0\right) U(s)\end{aligned} . \tag{2.39}$$

The transfer function from *u(t)* to *y(t)* is shown in

$$G(s) = \frac{Y(s)}{U(s)} = \frac{b_m s^m + b_{m-1}s^{m-1} + \ldots + b_1 s + b_0}{s^n + a_{n-1}s^{n-1} + \ldots + a_1 s + a_0} . \tag{2.40}$$

2.3 Routh–Hurwitz stability criterion

This section is based on [29] to introduce the basic theory of the Routh–Hurwitz stability criterion.

To determine the stability of linear time-invariant SISO systems, one simple way is to investigate the location of the roots of the characteristic equation of the system. The stable and unstable regions in the *s*-plane are shown in Figure 2.8 [29].

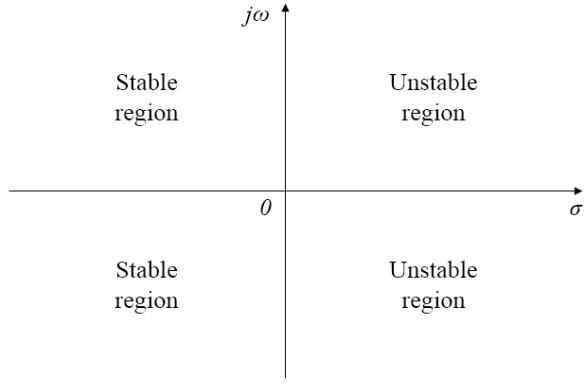

Figure 2.8. Stable and unstable regions in the *s*-plane ($s=\sigma+j\omega$)

For a linear time-invariant system which has a characteristic equation with constant coefficients, the Routh-Hurwitz criterion can analyze the stability by simply manipulating arithmetic operations. For a linear time-variant SISO system with a characteristic equation in the form of

$$F(s) = a_n s^n + a_{n-1}s^{n-1} + \ldots + a_1 s + a_0 = 0 , \tag{2.41}$$

the analysis process of Routh-Hurwitz criterion takes the following steps.

(1) Step one is to form the coefficients of the equation in (2.41) into the following tabulation:

$$\begin{array}{cccc} a_n & a_{n-2} & a_{n-4} & a_{n-6} & \ldots \\ a_{n-1} & a_{n-3} & a_{n-5} & a_{n-7} & \ldots \end{array}$$

(2) Step two is to obtain the Routh's tabulation (or Routh's array), which is illustrated here for a sixth-order equation:

$$a_6 s^6 + a_5 s^5 + \ldots + a_1 s + a_0 = 0 \,. \tag{2.42}$$

s^6	a_6	a_4	a_2	a_0
s^5	a_5	a_3	a_1	0
s^4	$\dfrac{a_5 a_4 - a_6 a_3}{a_5} = A$	$\dfrac{a_5 a_2 - a_6 a_1}{a_5} = B$	$\dfrac{a_5 a_0 - a_6 \times 0}{a_5} = a_0$	0
s^3	$\dfrac{A a_3 - a_5 B}{A} = C$	$\dfrac{A a_1 - a_5 a_0}{A} = D$	$\dfrac{A \times 0 - a_5 \times 0}{A} = 0$	0
s^2	$\dfrac{BC - AD}{C} = E$	$\dfrac{C a_0 - A \times 0}{C} = a_0$	$\dfrac{C \times 0 - A \times 0}{C} = 0$	0
s^1	$\dfrac{ED - C a_0}{E} = F$	0	0	0
s^0	$\dfrac{F a_0 - E \times 0}{F} = a_0$	0	0	0

(3) Step three is to determine the location of the roots by investigating the signs of the coefficients in the first column of the tabulation. If all the elements of the first column have the same sign, the roots of the equation are all in the left half of the *s*-plane, which is the stable region. Besides, the number of roots in the right half of the *s*-plane (unstable region) also can be obtained: it equals the number of changes of signs in the elements of the first column.

2.4 Nyquist stability criterion and describing function method

2.4.1 Nyquist stability criterion

This subsection is based on [29], for introducing the basic theory of the Nyquist stability criterion.

For a SISO system of which the closed-loop transfer function is

$$M(s) = \frac{G(s)}{1 + G(s)H(s)}, \tag{2.43}$$

the characteristic equation roots must satisfy

$$\Delta(s) = 1 + G(s)H(s) = 1 + L(s) = 0 . \tag{2.44}$$

Here, *L(s)* is the loop transfer function.

The Nyquist criterion determines the stability of a closed-loop system by analyzing the frequency-domain plots (the Nyquist plot) of the loop transfer function *L(s)*.

● Absolute stability:

The absolute stability is divided into the following two types. (1) Open-loop stability: if all the poles of the *L(s)* are in the left-half *s*-plane, the system is open-loop stable. (2) Closed-loop stability: if all the zeros of the 1+ *L(s)* or all the poles of the closed-loop transfer function are in the left-half *s*-plane, the system is closed-loop stable.

● Relative stability:

The relative stability indicates how stable the system is, which is measured by how close the Nyquist plot (or Nyquist curve) of *L(s)* is to the (-1, *j*0) point, in the frequency domain. The gain margin and phase margin are frequently used criteria for measuring relative stability of control systems. The detailed definitions of the gain margin and phase margin can be found in [29].

2.4.2 Describing function method for non-linear system

This subsection is based on [30], to introduce the basic theory of the stability analysis for non-linear system and the describing function method.

The describing function method is a common method to analyze the stability of non-linear systems, based on the Nyquist criterion. A system without external signals is taken as an example, the block diagram is shown in Figure 2.9 [30].

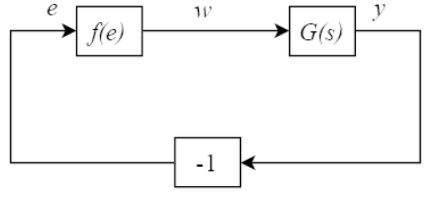

Figure 2.9. Block diagram for the describing function method

In the system, the *G(s)* is the transfer function of a linear part, the function *f* describes a static nonlinearity, and the input signal of *f* is assumed to be

$$e(t) = C\sin\omega t . \tag{2.45}$$

The output is a periodic function $w(t) = f(C\sin\omega t)$. By expanding this function into a Fourier series, the function *w* can be written in the form

$$w(t) = f(C\sin\omega t) = f_0(C) + A(C)\sin(\omega t + \phi(C)) + A_2(C)\sin(2\omega t + \phi_2(C)) + A_3(C)\sin(3\omega t + \phi_3(C)) + \ldots \quad (2.46)$$

For the fundamental component (with the angular frequency ω) the gain is given by $|G(i\omega)|$ and the change in phase by $\psi(\omega) = \arg G(i\omega)$.

Then, the complex number is defined as

$$Y_f(C) = \frac{A(C)e^{i\phi(C)}}{C}, \quad (2.47)$$

which is called the describing function of the nonlinearity. By introducing the Fourier coefficients

$$a(C) = \frac{1}{\pi}\int_0^{2\pi} f(C\sin\alpha)\cos\alpha d\alpha = A(C)\sin\phi(C), \quad (2.48)$$

$$b(C) = \frac{1}{\pi}\int_0^{2\pi} f(C\sin\alpha)\sin\alpha d\alpha = A(C)\cos\phi(C), \quad (2.49)$$

the complex number can be described as

$$Y_f(C) = \frac{b(C) + ia(C)}{C}. \quad (2.50)$$

The equations of the system can be described in the form

$$Y_f(C)G(i\omega) = -1, \quad (2.51)$$

which is an equation in the two unknowns C and ω. The solutions of the equation are the amplitude and frequency of an oscillation. No solution of the equation indicates that the system likely does not oscillate.

After rewriting (2.51) as

$$G(i\omega) = -\frac{1}{Y_f(C)}, \quad (2.52)$$

it is clearer that the solution can be interpreted as the intersection of two curves in the complex plane, namely the Nyquist curve $G(i\omega)$, plotted as a function of ω and $-1/Y_f(C)$, plotted as a function of C. An intersection of these two curves indicates the presence of an oscillation in the system [30].

An example from Paper V is shown in Figure 2.10. There is no intersection between the curves of the system (green curve) and dead zone (red dashed line), which means that the system is stable with the dead zone, under the Ep0 parameter settings. In contrast, the floating dead zone (red solid curve) leads to an oscillation in the system with the Ep3 parameter setting (blue curve); while when the system adopts the Ep0 setting, the oscillation is avoided.

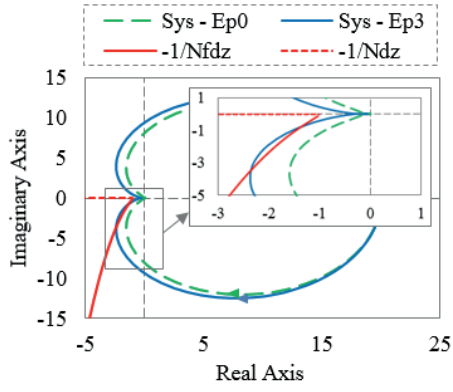

Figure 2.10. The Nyquist curve of the open-loop system under different governor parameters and the negative reciprocal of the describing functions. The describing functions in this figure are shown in (2.34) and (2.35).

3 Regulation quality and operating stability

The regulation quality and operating stability of HPPs are analyzed in this chapter. Firstly in section 3.1, a discussion on different operating conditions of HPPs is conducted, and the simulation performance of the TOPSYS model is presented. Then, grid-connected operation and isolated operation of HPPs are studied in section 3.2 and 3.3 respectively.

3.1 Different operating conditions of hydropower plants

This section is based on Paper III. The application of TOPSYS (in subsection 2.1.1) by comparing simulations with on-site measurement results is presented in this section, based on four engineering cases: one Swedish HPP (Case 1 shown in Figure 2.1) and three Chinese HPPs (case 2-4 shown in Figure 3.1). The aim of the model in TOPSYS is to achieve accurate simulation and analysis of different operation cases, e.g. small disturbance, large disturbance, start-up and no-load operation, etc.

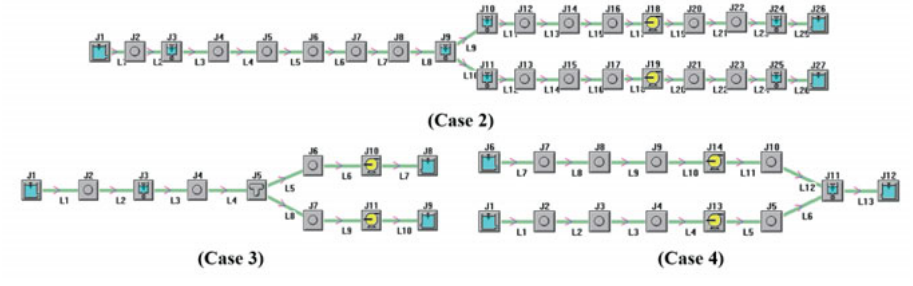

Figure 3.1. TOPSYS models of three Chinese HPPs with Francis turbines

The comparison between simulations and measurements for normal operation (small disturbances in grid-connected operation and isolated operation) are shown in Figure 3.2 through Figure 3.4. A good simulation in TOPSYS is a crucial basis of the studies in Paper I (grid-connected operation), Paper II (isolated operation) and Paper IV (grid-connected operation).

Overall, the simulation has a good agreement with the measurements. As shown in Figure 3.2, the effect of backlash is reflected: the GVO keeps stable for a short period during the direction change process (e.g. around 28

seconds). In Figure 3.3, after the frequency step change, the phenomenon of power reverse regulation caused by water hammer is simulated accurately, as well as the gradual power increase or decrease due to the surge (after 20 seconds). The oscillation after a load step change is examined by simulation and compared with the measurements, as shown in Figure 3.4. The simulation reflects the real operating condition well: under the power control mode in HPP Case 3, the power oscillates with the surge oscillation under certain governor parameter settings due to a relatively small cross section of the surge tank.

Other operation cases (large disturbance, start-up and no-load operation) are shown in Paper III. The results show that the model can yield trustworthy simulation results for different physical quantities of the unit under various operating conditions. The main error source of the simulation is the characteristic curves of the turbine, provided by manufacturers, which directly causes small deviations of power output and affects the rotation speed and pressure values. The reason might be that the characteristic curve does not really describe the on-site dynamic process accurately, and the error is especially obvious in the small-opening operation range. What's more, waterway system parameters might also have errors that impact the simulation.

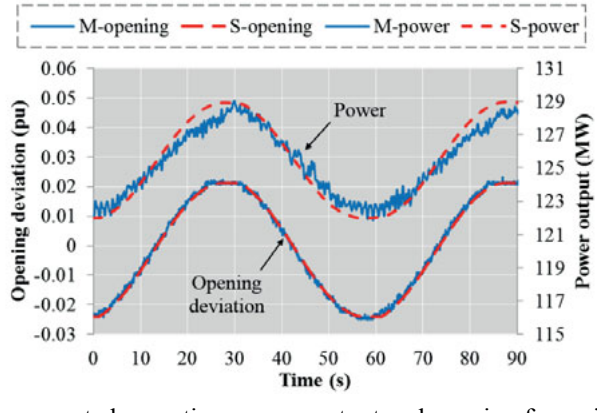

Figure 3.2. Grid-connected operation: power output and opening from simulation and measurement under sinusoidal frequency input (Case 1). In the figures of this thesis, the “M” refers to measurements and the “S” means simulation.

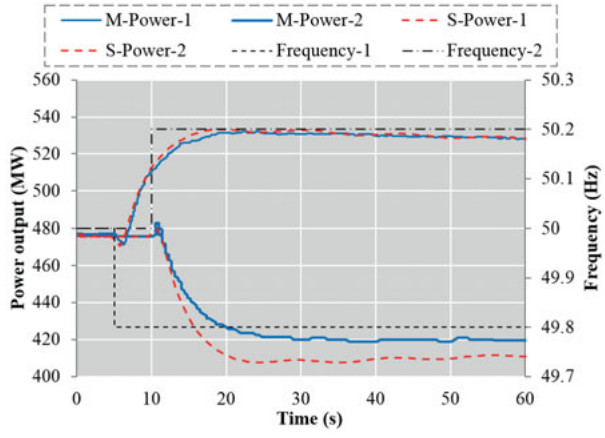

Figure 3.3. Grid-connected operation: power from simulation ("S-") and measurement ("M-") under step frequency input (Case 2).

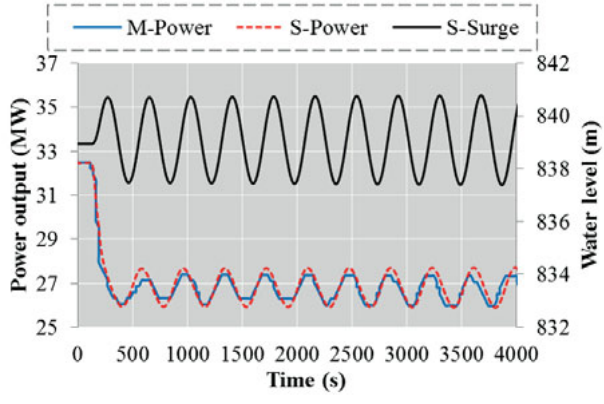

Figure 3.4. Isolated operation: Simulation ("S-") and measurement ("M-") of the power oscillation under power control mode (Case 3).

3.2 Response time for primary frequency control

This section is based on Paper I. The aim of this section is to investigate the general rules for controlling the power response time, based on the model in TOPSYS presented in subsection 2.1.1. The background, the test method and the specifications of primary frequency control can be found in Paper I.

The response time (deployment time) $T_{response}$ and the delay time T_{delay} of power response process are the key indicators in the thesis, as shown in Figure 3.5. The difference between the power response and the GVO response is the focus of the section.

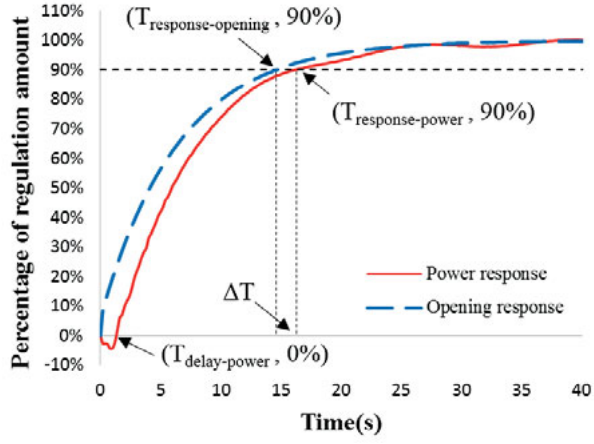

Figure 3.5. Illustration of different times under frequency step disturbance. The opening means guide vane opening (GVO).

Both theoretical analysis and numerical simulation are applied. Based on the theory in section 2.2, a time domain solution for guide vane opening response and a response time formula are deduced. The main variables of the formula are governor parameters, as shown in

$$T_1 = -\frac{1+b_p K_p}{b_p K_i} \ln\left[(1+b_p K_p - b_p K_i T_y)(1-\Delta)\right]. \tag{3.1}$$

Here, Δ is the target value (Δ is set to 90% according to [33]).

Then by applying the simulation based on the TOPSYS model in subsection 2.1.1, the factors which cause the time difference, between the power response time and the analytical response time of GVO, are investigated from aspects of both regulation and water way system. The power response time, T_4, can be expressed as

$$T_4 = T_1 + \Delta T = T_1 + \Delta T_1 + \Delta T_2 + \Delta T_3 . \tag{3.2}$$

The time difference ΔT (as shown in Figure 3.5), between the power response time (T_4) and the analytical response time of GVO (T_1), is mainly affected by the rate limiting and numerical algorithm (ΔT_1), the water hammer (ΔT_2) and the surge (ΔT_3).

The detailed methods and results are in Paper I. In the paper, the case 2 is investigated.

3.3 Frequency stability of isolated operation

This section is based on Paper II. The focus of this section is on stabilizing the low frequency oscillation of an isolated HPP caused by surge fluctuation.

3.3.1 Theoretical derivation with the Hurwitz criterion

Based on the simplified model in section 2.1.2 and the theory in section 2.3, a stability condition of frequency oscillation under frequency control and power control is obtained.

The stability region is the region which satisfies the stability condition in K_i-n coordinates by substituting the system parameters of different states into the stability condition. Here, n ($n = F/F_{th}$) stands for the coefficient of cross section area of the surge tank, where F and F_{th} are the real area and Thoma critical area [2], respectively.

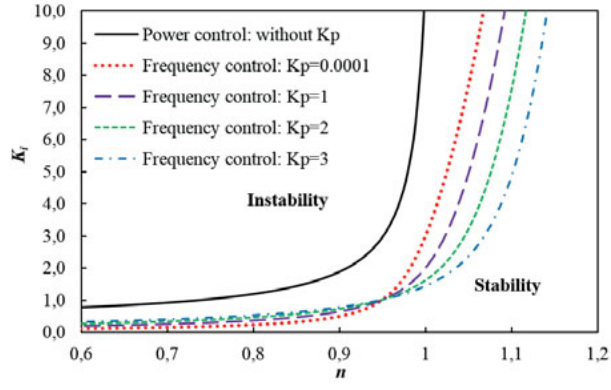

Figure 3.6. Stability region in K_i-n coordinates of two control modes

Based on the stability condition, a set of curves of stability region boundaries is achieved under two control modes, as shown in Figure 3.6. The stability region of power control is much larger than which of frequency control. There is no proportional gain (K_p can be regarded as 0) in power control, and it is conducive to the stability. However under frequency control, when K_p is set to near 0, the stability region is still smaller than for power control.

The detailed method and results are in Paper II.

3.3.2 Numerical simulation

Based on the TOPSYS model in subsection 2.1.1, numerical simulations on case 2 are applied to validate the result of the theoretical derivation. Results are shown in Figure 3.7 and Figure 3.8.

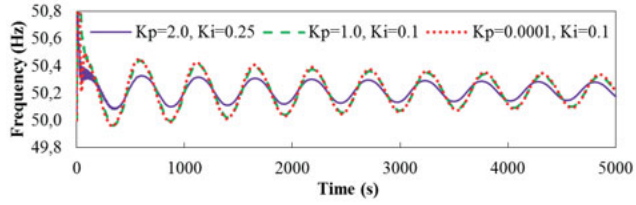

Figure 3.7. Frequency oscillation under frequency control with different governor parameters

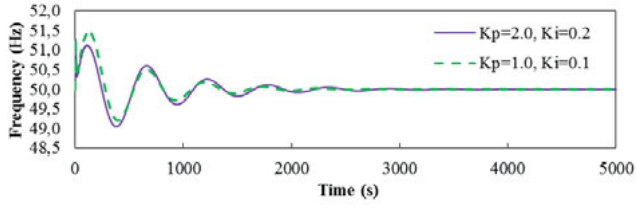

Figure 3.8. Frequency oscillation under power control with different governor parameters

From the simulation, the conclusion drawn in the theoretical derivation is verified: the power control produces a better effect on stability than the frequency control. More specifically, under the frequency control, it is hard to stabilize the frequency by adopting any of the three sets of parameters. Even when K_p is set to nearly 0, to compare with the power controller which is without proportion component ($K_p = 0$), the frequency instability still occurs. While under the power control, frequency stability is well ensured, and the contradiction between rapidity and stability is also indicated.

The detailed method, other results and discussion are in Paper II. Besides, it is necessary to have an additional discussion on the power control. The applying of the power control in the isolated operation condition is an ideal case, which cannot be implemented in the practical HPP operation. It is because that the load is unknown in reality, therefore the given power cannot be set properly. However, the conclusion based on the idealized case can supply the understanding and guidance for the stability in an islanded operation, which means the operation of a generating unit that is interconnected with a relatively small number of other generating units [34]. In the islanded system, some units operate in the frequency control mode to balance the changing peak load, and other units adopt the power control to maintain the stability. This issue is also a suggested topic for the future work.

4 Wear and tear

The wear and tear of hydropower turbines is the focus of this chapter. Firstly in section 4.1, the background, including practical engineering problems and several definitions in the study, are presented. Then, an investigation on the influence of PFC is presented in section 4.2. Based on the results, a controller filter is proposed in section 4.3 as a solution for reducing the wear of turbine and maintaining the regulation performance, reflected by the frequency quality of power systems.

4.1 Background

In terms of wear and tear of hydropower turbines, there are different views and corresponding indicators to evaluate. From a point of view of control, this study focuses on the movements of the guide vanes (GVs) in Francis turbines. The GV movements are expressed by the variations of guide vane opening (GVO). Two core indicators are discussed, as shown in Figure 4.1. The first is the movement distance which is the accumulated distance of GV movements; the second is the movement number which means the total number of movement direction changes. One movement corresponds to one direction change.

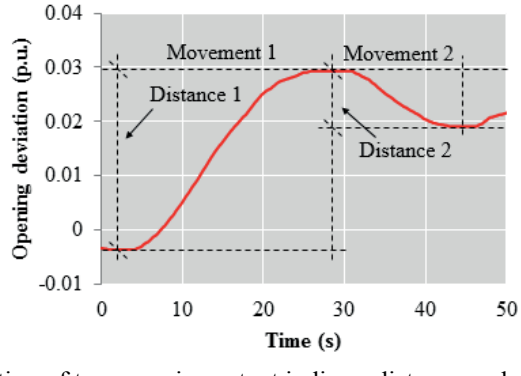

Figure 4.1. Illustration of two very important indices: distance and number of guide vane movement.

There is a balance to strike between the movement and power output, since a minimization of movement, and hence a minimization of cost for the owner of the unit, also implies a possible decrease of power response. Hence, blindly decreasing the movement is obviously not advisable. The balance is especially essential for large-distance movements, since each relatively large movement affects the regulation power needed by the power grid. However, the problem occurs on the small-distance movements: reference [35] found that during 4 months of observations in HPPs, between 75 and 90% of all GVO movements are less than 0.2% of full stroke. A simulation conducted in this study also demonstrates a similar result: 93.9% of all GVO movements are less than 0.2% of full stroke, as shown in Figure 4.2. More importantly, from the engineering experience, the wear and tear on the materials from small movements is believed to be more serious than from large movements. On the other hand, the regulation value from the small movements is not very obvious. Therefore, decreasing the number of small movements should be a priority.

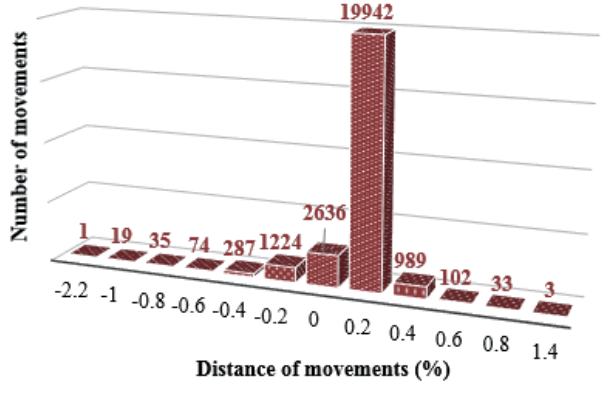

Figure 4.2. Histogram of simulated opening movements for real frequency record of a week in March, 2012. 19942 is the number of movements with the distance from 0 to 0.2%.

Small fluctuations of power system frequency, as a crucial reason for small GV movements, are discussed. In order to exemplify the characteristics of the Nordic power grid frequency, a one-day (24-hour) frequency measurement was conducted in Uppsala, on May 28th, 2015. The results are shown in Figure 4.3 and Figure 4.4.

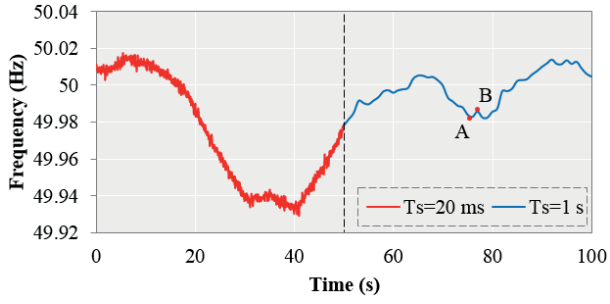

Figure 4.3. Time-domain illustration of small frequency fluctuations. *Ts* is the sampling time. The frequency change process from point A to B is a "frequency fluctuation", which is defined in this study.

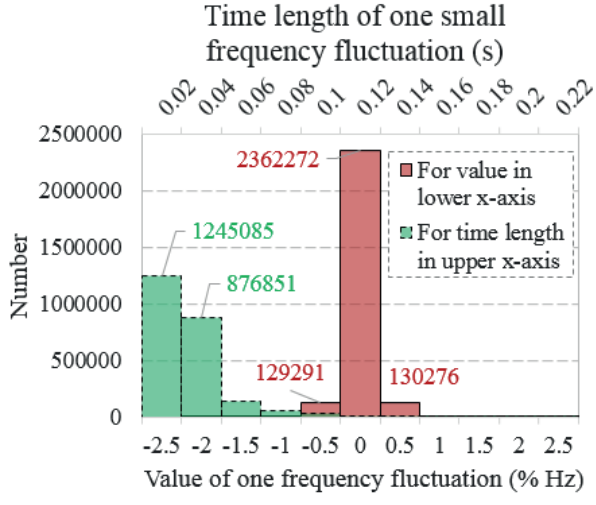

Figure 4.4. Histogram of values and time lengths of frequency fluctuations in the day. The sampling time of the frequency data is 0.02 ms. The total number of frequency fluctuations in this day is 2623711.

Figure 4.3 illustrates small frequency fluctuations, showing the data with two sampling times. One could have an intuition that, for the frequency changing process, direction variations happen every one or two sampling periods. The intuition is further verified by Figure 4.4, which demonstrates two important features: (1) the values of frequency fluctuations are mostly very small, within $\pm 2.5\times10^{-3}$ Hz which equals to 0.005% per unit (pu); (2) the time lengths of small fluctuations are also extremely small. All in all, these results indicate that the power system frequency indeed experiences fluctuations with small amplitude and high frequency. The small frequency fluctuation, as the input, would lead to the unfavorable amount of small GV movements.

More related data and discussions can be found in Paper IV and V.

4.2 Influence from primary frequency control

This section is based on Paper IV. The wear and tear on hydropower turbines due to PFC is studied, by applying numerical simulation and concise theoretical derivation.

Basic analytical formulas based on the idealized frequency deviation signals are presented. With the equation, the accumulated guide vane movement distance can be calculated for idealized sinusoidal input signal. Then, by adopting numerical simulations, the influences on guide vane movements by different factors are investigated. Governor parameters, power feedback mode and nonlinear factors in the governor (filters on the grid frequency signal) are analyzed based on ideal sinusoidal frequency input and real frequency records.

The detailed methods and results are in Paper IV. An important outcome is presented in the study: floating dead zone outperforms dead zone. The former not only reduces the overall movement distance, but also is more targeted on the more harmful small movements. It is an effective approach to decrease the wear and tear. As shown by the columns in Figure 4.5, by increasing the value of E_{fdz} and E_{dz}, the effects on decreasing the movement distance are similar. The main point is that the number of direction changes sharply decreased already with a tiny value (0.002 pu) of E_{fdz}, as shown by the scatters.

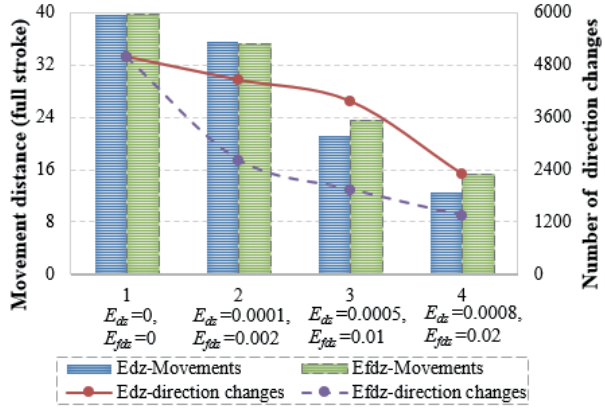

Figure 4.5. Movements and number of direction changes under different dead zone (E_{dz}) and floating opening dead zone (E_{fdz}) on the grid frequency signal, within one day in March, 2012

Based on this work, a further study on the controller filters and wear reduction was conducted, see section 4.3.

4.3 Controller filters for wear reduction considering frequency quality of power systems

This section is based on Paper V. Aiming at the aforementioned problem and the initial results on filters, this study proposes a solution which is applying a suitable filter in the turbine controller. However, the controller filters impact the active power output and then affects the power system frequency. Therefore, the purpose of this section is the trade-off between two objectives: (1) reducing the wear and tear of the turbines; (2) maintaining the regulation performance, reflected by frequency quality of power systems.

Different Simulink models are applied to investigate the guide vane movement, load disturbance and power system frequency, based on a one-day grid frequency data measured in this study. In the theoretical analysis, the describing functions and Nyquist criterion are adopted to examine the frequency response and stability of the system with different filters.

The detailed methods and results are in Paper V. The main conclusion is the features of different filters, as shown in Table 4.1. It suggests that the floating dead zone, especially the GVO filter after the controller, outperforms the widely-used dead zone on the trade-off between the wear reduction and frequency quality. In addition, the linear filter has a relatively weak impact on both GV movements and the frequency quality.

Table 4.1. Comparison between different filters

Filter	Advantages	Disadvantages
Dead zone	1. deceasing the GV movement distance effectively 2. no obvious influence on system stability	two fatal points: 1. worst frequency quality: the double-peaked distribution 2. not very effective in reducing the GV movement number, which is the main goal
Floating dead zone	1. well reducing both the GV movement numbers 2. deceasing the GV movement distance effectively 3. good frequency quality, especially with the GVO filter	might cause the limit circle oscillation (but it can be avoided, i.e. by tuning the governor parameters)
Linear filter	1. best frequency quality 2. can decrease both the movement distance and numbers to some extent	1. cannot obviously decrease both the movement distance and numbers 2. might cause the system instability (but it can be avoided, i.e. by tuning the governor parameters)

5 Conclusions

The main conclusions of the thesis are condensed in this chapter. Some of the conclusions are based on results that are only displayed in Paper I-V.

(1) For numerical modeling and different operating conditions of hydropower units, the following conclusions can be drawn:

● **The TOPSYS model is reliable for computing different physical quantities of the unit** (e.g. guide vane opening, active power, rotation speed, and pressures) by comparing the simulation with on-site measurements of different operating conditions, e.g. start-up, no-load operation, normal operation and load rejection in different control modes (frequency, opening and power feedback).

● **The main error source of the simulation might be the characteristic curves of the turbine, and the error is especially obvious in the small-opening operation range.** In the study, a better simulation for start-up process was obtained by changing the overall efficiency of characteristic curve. This simple method should be replaced by a more advanced and general one to adjust the simulation, as an important future work.

(2) For the response time for primary frequency control of hydropower units, the following conclusions can be drawn:

● The time difference ΔT, between the power response time and the analytical response time of opening, is mainly affected by **rate limiting and numerical algorithm (ΔT_1), water hammer (ΔT_2) and surge (ΔT_3).**

● **The most direct and effective method to control the response time is still adjusting the governor parameters.** Especially for a HPP without surge tank, the ΔT changes within a small range, so the formula of opening response time can also help to predict the power response and supply a flexible guidance of parameter tuning.

(3) For the frequency stability of an isolated hydropower plant with surge tank, the following conclusions can be drawn:

● **The power control has a better performance on frequency stability, comparing with the frequency control.** By contrast, power control leads to poorer rapidity.

● **The water inertia of final state is a key factor of frequency stability.** The worst operation case for stability is with large load, large load disturbance amplitude and low water head of the final state.

● For the operation case with small water inertia of final state, it is appropriate to adopt frequency control to ensure the stability and rapidity simultaneously. Otherwise, the power control can be applied to guarantee the stability at the expense of rapidity. Besides, the simulation also shows that if the instability already occurs under frequency control, the stability could be reobtained by manually switching the control mode to power control, although the frequency oscillation amplitude would increase temporarily during the switch-over transient process.

(4) For the influence from primary frequency control on wear and tear, the following conclusions can be drawn:

● **Parameter tuning is a key approach to affect the movements.** The theoretical formulas reflect the trend for real movements well, and they are effective to achieve a good estimate, even for power feedback mode.

● **The influence of the power feedback mode is normally not too large;** While comparing with opening feedback, increase or decrease of movements are both possible; The operation point affects the movements by changing of the ratio $\Delta y/\Delta p$. The surge normally does not cause much opening movement change, but it could lead to a "resonance".

● **Floating dead zone outperforms dead zone:** it not only reduces the overall movement distance, but also is more targeted on the more harmful small movements. It is an effective approach to decrease the wear and tear.

(5) For the study on controller filters, the following conclusions can be drawn:

● **The floating dead zone, especially the GVO filter after the controller, outperforms the widely-used dead zone on the trade-off between wear reduction and frequency quality. In addition, the linear filter has a relatively weak impact on both GV movements and the frequency quality.**

● The power system frequency experiences fluctuations with small amplitude and high frequency, which is a crucial cause of small GV movements.

● Without any artificial filters, the majority of the frequency fluctuations are inherently filtered by the actuator in the governor system.

● A relatively long sampling time (1 s) is valid for further simulations, without bringing much influences on the results.

6 Future work

The content of my future research is in the following respects:

(1) Hydraulic - mechanical- electrical -magnetic coupling mode and oscillation mechanism: In the first stage of my PhD program (before the Licentiate examination), the electrical part of the system model is relatively simple. In the next stage, I will establish a high-order refined mathematical model, considering more factors in generators and power systems, for analyzing the hydraulic - mechanical- electrical – magnetic coupling mode and the coupling oscillation of the multiple physical quantities. This would be the main challenge and the basis of my future work.

(2) Active power control of HPPs for frequency stability of power systems: I will explore the joint operating effect between the HPPs and high-frequency generator tripping or low-frequency load shedding, for large disturbance issues of grid frequency. For the wear and tear issue, I will further explore the optimization control strategies and filter settings, by applying long-term simulations and frequency-domain analysis on the closed-loop systems.

(3) Reactive power control strategy of HPPs for the voltage and rotor angle stability of power systems: I will analyze the low voltage ride through (LVRT) ability of the hydropower units under different operating conditions and coupling modes, optimize the set-up and performance of automatic voltage regulator (AVR). Furthermore, the dynamic response of HPPs under the local mode, the inter-regional mode and the control mode of rotor angle oscillation will be investigated. The design and parameter setup of power system stabilizer (PSS) will be optimized and the operating control strategy that satisfies rotor angle stability requirements will be proposed.

In terms of the research method:

(1) I will continue to develop the software TOPSYS, and mainly focus on extension of the electrical components. MATLAB/Simulink will still be applied, especially for the frequency-domain analysis and the study from the perspective of the whole power system. Simulation and analysis in PSAT, an open-source software for power system analysis, is currently also under consideration. Appropriate time-domain, frequency-domain and analytical calculation methods will be explored.

(2) In order to validate the reliability of theoretical analysis and numerical simulation, more experiments will be conducted, e.g. on the hydro generator

experiment setup at Uppsala University and the experiment hall for physical models of pumped storage power plants at Wuhan University in China.

It is worth mentioning that some details of suggested future work can be found in the discussion or conclusions section in Paper I - V.

7 Summary of papers

Paper I

Response Time for Primary Frequency Control of Hydroelectric Generating Unit

The aim of this paper is to build a suitable model for conducting reliable simulation and to investigate the general rules for controlling the power response time.

Two huge hydropower plants with surge tank from China and Sweden are considered in the simulation of step tests of primary frequency control, and the results are validated with data from full scale measurements. From the analytical aspect, this paper deduces a time domain solution for guide vane opening response and a response time formula, of which the main variables are governor parameters. Then, the factors which cause the time difference, between the power response time and the analytical response time of opening, are investigated from aspects of both regulation and water way system.

It is demonstrated that the formula can help to predict the power response and supply a flexible guidance of parameter tuning, especially for a hydropower plant without surge tank.

The author performed the theoretical analysis, simulations and wrote the paper.

Paper II

Frequency Stability of Isolated Hydropower Plant with Surge Tank under Different Turbine Control Modes

The focus of this paper is on stabilizing the low frequency oscillation of an isolated HPP caused by surge fluctuation.

From a new perspective of HPP operation mode, frequency stability under power control is investigated and compared with frequency control, by adopting the Hurwitz criterion and numerical simulation. In a theoretical derivation, the governor equations of frequency control and power control are introduced to the mathematical model. For numerical simulation, a governor model with control mode switch-over function is built. The frequency oscillations under frequency control, power control and control mode switch-over are simulated and investigated respectively, with different governor parameters and operation cases.

The result shows that the power control has a better performance on frequency stability at the expense of rapidity, comparing with the frequency control. Other recommendations regarding worst operation cases and choice of control modes are also developed.

The author performed the simulation and discussions, and wrote the manuscript.

Paper III

A Mathematical Model and Its Application for Hydro Power Units under Different Operating Conditions

This paper presents a mathematical model of hydropower units, especially the governor system model for different operating conditions, based on the basic version of the software TOPSYS.

The mathematical model consists of eight turbine equations, one generator equation, and one governor equation, which are solved for ten unknown variables. The generator and governor equations, which are different under various operating conditions, are presented and discussed in detail. All the essential non-linear factors in the governor system (dead-zone, saturation, rate limiting and backlash) are also considered. Case studies are conducted based on one Swedish hydropower plant and three Chinese plants. The simulation and on-site measurements are compared for start-up, no-load operation, normal operation and load rejection in different control modes (frequency, opening and power feedback). The main error in each simulation is also discussed in detail.

As a result, the model application is trustworthy for simulating different physical quantities of the unit (e.g. guide vane opening, active power, rotation speed, and pressures at volute and draft tube). The model has already been applied effectively in consultant analyses and scientific studies.

The author performed programming works, simulations and discussions, and wrote the paper.

Paper IV

Wear and Tear on Hydro Power Turbines – Influence from Primary Frequency Control

Nowadays the importance and need of primary frequency control of hydropower units are significantly increasing, because of the greater proportion of intermittent renewable energy sources and more complex structure of power systems. It brings a problem of increasing wear and tear of turbines.

This paper studies this problem by applying numerical simulation and concise theoretical derivation, from the point of view of regulation and control. Governor models under opening and power feedback mode are built and validated by measurement data. The core indicator, guide vane movement, is analyzed based on ideal sinusoidal frequency input and real frequency rec-

ords. The results show the influences on wear and tear of different factors, e.g. governor parameters, power feedback mode and nonlinear governor factors.

The author deduced the theory formula, performed the simulations and analysis, and wrote the manuscript.

Paper V

Wear reduction for hydro power turbines considering frequency quality of power systems: a study on controller filters

In this paper, the controller filter is proposed as a solution of the trade-off between reducing the wear of turbine and maintaining the regulation performance, reflected by the frequency quality of the power systems.

The widely-used dead zone is compared with floating dead zone and linear filter, by time domain simulation and frequency domain analysis. The position of the filter in the governor system, i.e. before or after the controller, is also discussed. Different Simulink models are applied to investigate the guide vane movement, load disturbance and power system frequency, based on a one-day grid frequency data measured in this study. In the theoretical analysis, the describing functions and Nyquist criterion are adopted to examine the frequency response and stability of the system with different filters.

The results show that the floating dead zone, especially the one after the controller, has a better performance than the dead zone on both the wear reduction and frequency quality. The linear filter has a relatively weak impact on both guide vane movements and the frequency quality. Other related conclusions and understandings are also obtained.

The author engaged in the measurements, performed the theoretical analysis and simulations, and wrote the manuscript.

8 Acknowledgements

Firstly, I would like to express my sincere gratitude to my main supervisor Per Norrlund, for your great guidance, for your rich scientific knowledge and engineering experience, for your rigorous attitude towards work and kind encouragement to me. To my associate supervisor Urban Lundin, thank you so much for your guidance of my research and support of the collaboration with the Chinese group!

My fellow hydropower group members in Uppsala: Johan Bladh, Linn Saarinen, Johan Abrahamsson, Birger Marcusson, Jose Perez, Jonas Noland, Fredrik Evestedt, thank you for your support and inspirations to my research. Especially to my co-author, Linn Saarinen, thank you a lot for your comments and discussion on my works, and teaching me a lot regarding systems and control.

I would like to thank my collaborators in Wuhan University in China. Thank you Prof. Jiandong Yang, although you are not my "official" supervisor any more, but your support and guidance is really helpful and always highly appreciated. To my co-authors and friends in the hydropower group in Wuhan, especially Wencheng Guo, Chao Wang and Wei Zeng, thank you for your discussion and help on my research, and I also admire your great effort and performance on your studies.

To the SVC reference group, really thank you for your discussions, comments and supports to my project. To Prof. Mats Leijon, thank you for accepting me as a PhD student and helping me to get my PhD scholarship. To Thomas Götschl, thank you for your support on my computer. Thank you, Maria Nordengren, Gunnel Ivarsson, Ingrid Ringård and Anna Wiström, for the really helpful administrative works. All my friends, lunch-mates and colleges in the Division of Electricity, thank you for your company and sharing your interesting everyday life and various knowledge. My sincere thanks also go to all my Chinese friends in Uppsala, for all the happiness we shared and all the delicious Chinses food we had together!

I would like to sincerely thank the financial support of my projects: China Scholarship Council (CSC), StandUp for Energy, Swedish Hydropower Centre (SVC) and Anna Maria Lundin's scholarship committee.

Finally, I give my special thanks to my family and my girlfriend, my gratefulness to you is beyond description!

9 Svensk sammanfattning

Vattenkraft spelar en viktig roll genom att bidra till säker, stabil och effektiv drift av storskaliga elektriska kraftsystem. Vattenkraftverkens prestanda vad beträffar frekvensreglering blir allt viktigare. Slitaget på vattenturbinerna har ökat under senare år, på grund av ett ökande reglerarbete till följd av en fortsatt integration av intermittenta förnybara energikällor. Forskning om slitage på vattenkraftaggregat är följaktligen synnerligen viktigt.

En sofistikerad modell av vattenkraftaggregat presenteras. Numeriska simuleringar för olika driftfall jämförs med mätresultat från ett svenskt och tre kinesiska kraftverk. De huvudsakliga avvikelserna för varje fall diskuteras också i detalj. Därefter undersöks generella samband för hur man kan styra responstiden för uteffekten vid nätansluten drift. En formel härleds för att förutsäga svarstiden och för att ge en flexibel vägledning vid parametrering av turbinregulatorn. Faktorer som påverkar svarstiden undersöks, kopplat både till reglering och till vattenvägar. Lågfrekventa oscillationer orsakade av svallning undersöks för önätsdrift. Frekvensstabilitet vid effektreglering jämförs med frekvensreglering genom applicering av Hurwitz stabilitetskriterium och med hjälp av numeriska simuleringar.

Vad beträffar slitage av vattenturbiner presenteras en omfattande diskussion om inverkan av primärreglering, utifrån numeriska simuleringar och en kortfattad teoretisk härledning. Resultaten visat inverkan av faktorer som regulatorparametrar, effektåterkoppling och ickelineariteter kopplade till regulatorn. Därefter föreslås filtrering i regulatorn som en lösning på avvägningen mellan reducering av turbinslitage och upprätthållande av reglerprestanda, vilken speglas av frekvenskvaliteten hos kraftsystemet ifråga. Det vanligt förekommande dödbandet jämförs med ett flytande dödband och ett linjärt filter, både genom tidsupplösta simuleringar och genom spektralanalys.

Resultaten bidrar med förståelse av modelleringen och analysen av dynamiska förlopp i vattenkraftsystem och med förslag rörande reglerstrategier för vattenkraftverk i olika driftsituationer som underkastas stabilitetskrav från kraftsystemdrift.

10 References

[1] F. Demello, R. Koessler, J. Agee, P. Anderson, J. Doudna, J. Fish*, et al.*, "Hydraulic-turbine and turbine control-models for system dynamic studies," *IEEE Transactions on Power Systems,* vol. 7, pp. 167-179, 1992.

[2] E. D. Jaeger, N. Janssens, B. Malfliet, and F. V. D. Meulebroeke, "Hydro turbine model for system dynamic studies," *IEEE Transactions on Power Systems,* vol. 9, pp. 1709-1715, 1994.

[3] O. S. Jr, N. Barbieri, and A. Santos, "Study of hydraulic transients in hydropower plants through simulation of nonlinear model of penstock and hydraulic turbine model," *IEEE Transactions on Power Systems,* vol. 14, pp. 1269-1272, 1999.

[4] H. Fang, L. Chen, N. Dlakavu, and Z. Shen, "Basic modeling and simulation tool for analysis of hydraulic transients in hydroelectric power plants," *IEEE Transactions on Energy Conversion,* vol. 23, pp. 834-841, 2008.

[5] Y. Zeng, Y. Guo, L. Zhang, T. Xu, and H. Dong, "Nonlinear hydro turbine model having a surge tank," *Mathematical and Computer Modelling of Dynamical Systems,* vol. 19, pp. 12-28, 2013.

[6] B. Strah, O. Kuljaca, and Z. Vukic, "Speed and active power control of hydro turbine unit," *IEEE Transactions on Energy Conversion,* vol. 20, pp. 424-434, 2005.

[7] C. Nicolet, B. Greiveldinger, J.-J. Hérou, B. Kawkabani, P. Allenbach, J.-J. Simond*, et al.*, "High-order modeling of hydraulic power plant in islanded power network," *IEEE Transactions on Power Systems,* vol. 22, pp. 1870-1880, 2007.

[8] C. Nicolet, "Hydroacoustic modelling and numerical simulation of unsteady operation of hydroelectric systems," École Polytechnique Fédérale de Lausanne, 2007.

[9] S. Mansoor, D. Jones, D. A. Bradley, F. Aris, and G. Jones, "Reproducing oscillatory behaviour of a hydroelectric power station by computer simulation," *Control Engineering Practice,* vol. 8, pp. 1261-1272, 2000.

[10] J. I. Pérez-Díaz, J. I. Sarasúa, and J. R. Wilhelmi, "Contribution of a hydraulic short-circuit pumped-storage power plant to the load–frequency regulation of an isolated power system," *International Journal of Electrical Power & Energy Systems,* vol. 62, pp. 199-211, 2014.

[11] N. Kishor, R. Saini, and S. Singh, "A review on hydropower plant models and control," *Renewable and Sustainable Energy Reviews,* vol. 11, pp. 776-796, 2007.

[12] G. A. Munoz-Hernandez, S. a. P. Mansoor, and D. I. Jones, *Modelling and Controlling Hydropower Plants*: Springer, 2013.

[13] S. Wei, *Water Turbine Regulation (In Chinese)*. Wuhan: Huazhong University of Science and Technology Press, 2009.

[14] L. Fu, "Research on governing quality and stability of the hydropower station with surge tank (In Chinese)," Doctor, Wuhan University, Wuhan, 2009.

[15] H. Bao, "Research on setting condition of surge chamber and operation control of the hydropower station (In Chinese)," Doctor, Water Resources and Hydropower Engineering, Wuhan University, Wuhan, 2010.
[16] L. Saarien, "A hydropower perspective on flexibility demand and grid frequency control," Licentiate, Department of Engineering Sciences, Uppsala University, Uppsala, 2014.
[17] D. Chen, C. Ding, Y. Do, X. Ma, H. Zhao, and Y. Wang, "Nonlinear dynamic analysis for a Francis hydro-turbine governing system and its control," *Journal of the Franklin Institute,* vol. 351, pp. 4596-4618, 2014.
[18] M. E. Cebeci, U. Karaağaç, O. B. Tör, and A. Ertaş, "The effects of hydro power plants' governor settings on the stability of Turkish power system frequency," presented at the ELECO Conf, 2007.
[19] H. V. Pico, J. D. McCalley, A. Angel, R. Leon, and N. J. Castrillon, "Analysis of Very Low Frequency Oscillations in Hydro-Dominant Power Systems Using Multi-Unit Modeling," *IEEE Transactions on Power Systems,* vol. 27, pp. 1906-1915, 2012.
[20] M. Grøtterud, "Analysis of the Slow Floating in Grid Frequency of the Nordic Power System: Impact of Hydraulic System Characteristics," Master, Department of Electric Power Engineering, Norwegian University of Science and Technology, 2012.
[21] J. Ukonsaari, "Wear and friction of synthetic esters in a boundary lubricated journal bearing," *Tribology international,* vol. 36, pp. 821-826, 2003.
[22] R. Gawarkiewicz and M. Wasilczuk, "Wear measurements of self-lubricating bearing materials in small oscillatory movement," *Wear,* vol. 263, pp. 458-462, 2007.
[23] G. F. Simmons, "Journal bearing design, lubrication and operation for enhanced performance," Doctor, Luleå University of Technology, 2013.
[24] M. Gagnon, S. Tahan, P. Bocher, and D. Thibault, "Impact of startup scheme on Francis runner life expectancy," in *IOP Conference Series: Earth and Environmental Science*, 2010, p. 012107.
[25] E. Doujak, "Effects of Increased Solar and Wind Energy on Hydro Plant Operation," *HRW-Hydro Review Worldwide,* 2014.
[26] C. Trivedi, B. Gandhi, and C. J. Michel, "Effect of transients on Francis turbine runner life: a review," *Journal of Hydraulic Research,* vol. 51, pp. 121-132, 2013.
[27] P. Storli and T. Nielsen, "Dynamic load on a Francis turbine runner from simulations based on measurements," in *IOP Conference Series: Earth and Environmental Science*, 2014, p. 032056.
[28] U. Seidel, C. Mende, B. Hübner, W. Weber, and A. Otto, "Dynamic loads in Francis runners and their impact on fatigue life," in *IOP Conference Series: Earth and Environmental Science*, 2014, p. 032054.
[29] F. Golnaraghi and B. Kuo, *Automatic control systems*, 2010.
[30] A. Gelb and W. E. V. Velde, *Multiple-input describing functions and nonlinear system design*: McGraw-Hill, New York, 1968.
[31] H. Bao, J. Yang, and L. Fu, "Study on Nonlinear Dynamical Model and Control Strategy of Transient Process in Hydropower Station with Francis Turbine," in *Power and Energy Engineering Conference, 2009. APPEEC 2009. Asia-Pacific*, 2009, pp. 1-6.
[32] L. Saarinen and U. Lundin, "Robust PI design for primary frequency control of a power system dominated by hydropower (unpublished results)."
[33] DL/T 1040-2007 -The grid operation code, 2007.

[34] IEEE Guide for the Application of Turbine Governing Systems for Hydroelectric Generating Units, IEEE Std 1207-2004, 2004.
[35] J. A. Jones, R. A. Palylyk, P. Willis, and R. A. Weber, "Greaseless Bushings for Hydropower Applications: Program, Testing, and Results," US Army Corps of Engineers, Engineer Research and Development Center1999.